Desalination and Water Treatment
www.deswater.com

doi: 10.5004/dwt.2022.28646

266 (2022) 202–211
August

Removal of methyl orange from aqueous solution by electrochemical process using stainless steel/PbO_2-TiO_2 stable electrode

Tot T. Pham[a,b,c], Thuy T.T. Mai[a,b], Binh T. Phan[a,b,*]

[a]*Institute of Chemistry, Vietnam Academy of Science and Technology, 18 Hoang Quoc Viet, Cau Giay, Hanoi, Vietnam, Tel. +84-2437-564312; Fax: +84-2438-361283; emails: phanthibinh@ich.vast.vn/phanthibinh.ich@gmail.com (B.T. Phan), totpt@hict.edu.vn (T.T. Pham), thuyttmai1980@gmail.com (T.T.T. Mai)*
[b]*Graduate University of Science and Technology, Vietnam Academy of Science and Technology, 18 Hoang Quoc Viet, Cau Giay, Hanoi, Vietnam*
[c]*Faculty of Yarn-Textile Technology, Hanoi Industrial Textile Garment University, Le Chi, Gia Lam, Hanoi, Vietnam*

Received 9 December 2021; Accepted 1 June 2022

ABSTRACT

Methyl orange (MO) belongs to the group of acid dyes with an azo chromophore. It is a toxic substance that harms human health and the environment. Therefore, it is very necessary to treat MO before discharged into environment. In this paper, the sol–gel TiO_2 nanoparticles were dopped into PbO_2 layer on stainless steel (SS) substrate by the cyclic voltammetry method. The obtained SS/PbO_2-TiO_2 composite electrode was used to remove MO from the aqueous solution. The effects of current density, initial pH, degradation time, and MO concentration were investigated. The results by X-ray diffraction showed that the β-PbO_2 co-existed with α-PbO_2 in composite coating. TiO_2 particles have been successfully doped into the PbO_2 layer because of containing 0.3% Ti proven by energy dispersive X-ray spectroscopy examination. The optimal conditions for MO treatment were a current density of 1.75 mA cm^{-2}, initial pH of 6, degradation time of 50 min, and MO concentration of 50 mg L^{-1}. The decolorization efficiency reached 99.31%, indicating that the MO was almost completely removed in the aqueous solution by electrocatalytic oxidation method using the stable electrode SS/PbO_2-TiO_2 as the anode.

Keywords: PbO_2-TiO_2 composite; Electrocatalytic oxidation; Methyl orange; Colorant treatment

1. Introduction

Along with economic development, the problem of environmental pollution is increasingly serious, including the problem of water pollution. One of the most common types of pollutants is dyes. Dyes have entered the water resources from different industries such as textile, food, cosmestic, plastic, paper and printing [1–3]. The wastewater of the industries cause serious environmental pollution and affect human health. If the content of dyes in water is high, it will affect the growth and development of aquatic species because the ability to regenerate oxygen and absorb sunlight is reduced [4]. Among the dyes, methyl orange (MO) is also interested in research by many scientists because it is toxic to aquatic life and human health. MO ($C_{14}H_{14}N_3NaO_3S$) belongs to acid dyes group with stability azo chromophore (–N=N–). Generally, MO is difficult to remove due to high water solubility and low biodegradability [5]. Currently, there are many methods to removal dyes in wastewater such as adsorption [3,6], coagulation–flocculation [7], biological treatment [8], chemical adsoption [9], bioadsorption [10], sonophotocatalytic treatment [11], Fenton reaction [12], electrocoagulation [13], and electrocatalytic oxidation [1,14]. Each method has advantages and disadvantages as well.

* Corresponding author.

Biological treatment proven technology and cost-effective but it has some limitations such as requiring a greater time for functioning, a little flexibility in design and operation [15]. Adsorption methods convert pollutants into another form [12]. Coagulation and flocculation create a lot of sludge [3]. But the electrocatalytic oxidation method has many significant advantages such as easy operation, laboratory temperature and pressure, high degradation efficiency, and no secondary pollution generation [16–19]. However, besides these advantages, there are still some limitations such as the short life of electrodes and low surface to volume ratio [19]. The mechanism of oxidation organic matter can be described is as follows: First, H_2O discharged at the anode surface (AS) to create AS($OH^•$). Then, organics are oxidized by hydroxyl radicals AS($OH^•$) to form CO_2 and H_2O [1,20–22] describing the mechanism of electrocatalysis occurring simply on the electrode surface as shown in Fig. 1.

Parameters of reaction time, pH value, concentration of organic substances and current density all have great influence on the efficiency of the electrooxidation process [23,24]. However, the anode electrode material plays a very important role in the electrochemical process, contributing to improving the MO processing efficiency [1]. The anode materials used for the electrochemical degradation process must be inert ones such as G/β-PbO_2 [1], Ti/PbO_2 [25], Ti/SnO_2-Sb_2O_3/PbO_2-ZrO_2 [16], Nb/PbO_2 [18], G/Ti_4O_7 [14], SS/2D-PbO_2 [26], Ti/SnO_2-Sb/PbO_2-TiO_2 [27]. Ti/SnO_2-Sb_2O_3/PbO_2-TiO_2 [28]. Thus, the PbO_2-TiO_2 coating is mainly studied on the Ti substrate that has already been coated with another mixed oxide layer. PbO_2-TiO_2 composite could be synthesized by various ways such as electrode position by constant current method [29–32] and thermal combined electrochemical technique [28,29]. In the combined method, the authors first synthesized the metal oxide layers (SnO_2-Sb, SnO_2-Sb_2O_3) on the substrate by thermal method, then continued to superimpose PbO_2-TiO_2 layers by electrochemical method. These composite electrodes have a more stable structure and longer life than the original PbO_2 electrode [28]. MO treatment efficiency reached 95.5% after 240 min processing, quite high compared to some other processing methods such as combining hydrodynamic cavitation and chlorine dioxide (90.5% after reaction time of 90 min) [33], and electrocoagulation (83.0% after 15 min processing) [13]. However, a fabrication of this composite direct on stainless steel (SS) substrate by electrochemical method has not been mentioned much. Based on the literature review, there have been no reports on the SS/PbO_2-TiO_2 stable electrode fabricated by cyclic voltammetry (CV) method using for anode material to remove MO from wastewater. The potential scanning speed as well as the number of potential scan cycles are two parameters that have a great influence on the quality and thickness of the electrochemical coating [34]. Moreover, this synthesis method is both simple, easy to perform and less expensive because the composite layer is formed directly on the SS substrate in just one step. Therefore, the fabrication of SS/PbO_2-TiO_2 electrode was regarded in this study.

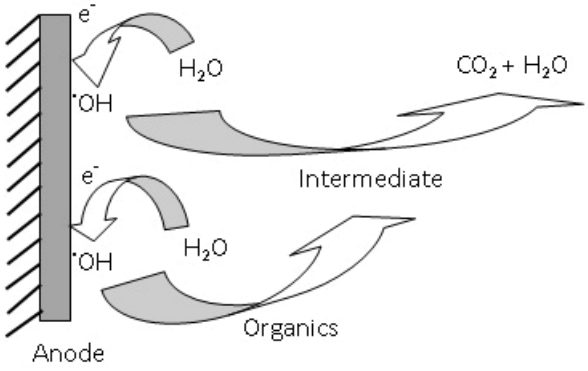

Fig. 1. Simulation of the MO decomposition pathway mechanism on the anode.

In this paper, SS/PbO_2-TiO_2 electrode was prepared by CV method at constant scan rate and with unchanged CV number. Then, the electrode was used to treat MO in wastewater by the constant current method. The optimal parameters such as current density, initial pH, degradation time and MO concentration in the treatment process were also investigated. Easy SS/PbO_2-TiO_2 stable electrode fabrication by CV method and very high MO processing efficiency are the highlights of this research.

2. Experimental

2.1. Chemicals

All chemicals were analytical grade from China (nitric acid (65%–68%), copper(II) nitrate trihydrate (>99%), sodium hydroxide (>99%), methyl orange (>99%)) and Germany (Lead nitrate (>99%), ethylene glycol (>99%)). TiO_2 nanoparticles were performed in sol–gel form (50 g L^{-1}).

2.2. Preparation and characterization of PbO_2-TiO_2 composite electrode

Before synthesizing the SS/PbO_2-TiO_2 electrode, the SS substrate of 0.283 cm^2 needs to be cleaned and polished. It was first polished on sandpaper from 400 to 2000, then dipped in a washing solution (concentrated H_2SO_4 plus $K_2Cr_2O_7$) to remove impurities. Finally, the electrode was treated in 60 g L^{-1} NaOH solution for electrochemical polishing by CV method (scan rate of 200 mV s^{-1}, potential from –0.7 to 0.5 V). PbO_2-TiO_2 composite was synthesized directly on clean SS by CV method from a mixed solution (0.5 M $Pb(NO_3)_2$, 0.05 M $Cu(NO_3)_2$, 0.1 M HNO_3, 0.1 M $C_2H_6O_2$, and 2 g L^{-1} TiO_2). The conditions for this step were scan rate of 50 mV s^{-1}, 300 cycles, and voltage range from 1.2 to 1.7 V vs. Ag/AgCl, sat. KCl reference electrode.

The surface morphology of SS/PbO_2-TiO_2 composite electrode was examined by scanning electron microscope (SEM) on Hitachi S-4800 (Japan). Material properties were obtained by X-ray diffraction (XRD) and energy dispersive X-ray spectroscopy (EDS) on D8-ADVANCE (Germany) and Jeol JSM-6490 JED 2300 (Japan), respectively. The electrochemical property of this composite electrode was characterized by CV (0.5 M H_2SO_4 measuring solution, potential region from 0.8 to 1.8 V, scan rate of 100 mV s^{-1}) and potential polarization (scan rate of 5 mV s^{-1}, potential from –200 to 200 mV compared to open circuit voltage (OCP) methods.

2.3. Treatment of MO and analytical method

MO in water was treated on a three-electrode system, including counter electrode (platinum plate), working electrode (SS/PbO_2-TiO_2 composite electrode), and reference electrode (Ag/AgCl, sat. KCl electrode). The electrolyte solution included 0.08 M Na_2SO_4, initial pH (varied from 5 until 11), and initial MO concentration (30, 50, 70, 90, and 110 mg L^{-1}). The further parameters for MO degradation were current density (1.00, 1.25, 1.50, 1.75, and 2.00 mA cm^{-2}), and treatment time (10, 20, 30, 40, 50, and 60 min). The volume of MO solution was 10 mL for each experiment. MO solution before and after the degradation were measured by UV-Vis on the S80 (England) to determine the removal efficiency (H). In our experience, the color absorbance only has good linearity in the low concentration range (2–10 mg L^{-1}). Therefore, this concentration range was chosen to construct a calibration curve to detect the concentration of MO in solutions. Absorbance was read at 465 nm. If the color of the MO solution is too concentrated, it should be diluted before the UV-Vis measurement is performed to obtain more accurate results.

The H value was determinate according to the following equation:

$$H = \frac{(C_0 - C_t)}{C_0} \times 100 \quad (1)$$

where C_0 is the initial MO concentration and C_t is the residual MO concentration of solution after a time of MO treatment. C_t is determined using the previously established calibration curve.

The analysis of intermediates obtained from the degradation of MO was determined by high-pressure liquid chromatography-mass spectrometry (HPLC/MS) on the Agilent 6530 Accurate-Mass QTOF (United States). Oxidation–reduction potential (ORP) was measured by using Sension1 unit (HACH, USA). It describes the degree of MO solution treatment.

3. Results and discussion

3.1. Physical characteristics of PbO_2-TiO_2 composite electrode

3.1.1. X-ray diffraction

Fig. 2 is the XRD spectrum of PbO_2-TiO_2 composite. The diffraction peaks located at 2θ of 25.5°, 32.0°, 36.2°, 49.0°, 52.1°, 54.1°, 59.0°, 62.5°, 62.5° and 66.8° are featured the β-PbO_2 form. The weak peaks located at 2θ of 30.0°, 49.5° and 56.0° demonstrated the presence of α-PbO_2 form [18,26]. This shows that PbO_2 in the composite exists in both crystalline forms.

3.1.2. EDS study

The surface composition analysis of SS/PbO_2-TiO_2 composite electrode was performed by EDS spectrum. It is seen in Fig. 3 that Pb, O and Ti elements can be detected in the PbO_2-TiO_2 composite [29]. The composition of elements in the composite is shown in Table 1. The result of EDS analysis indicated that the TiO_2 was successfully doped into PbO_2 coating by the CV method thanks to the contribution of 0.3% Ti besides O and Pb.

3.1.3. SEM observation

The surface morphology of SS/PbO_2 and SS/PbO_2-TiO_2 composite electrodes was investigated by SEM as shown in Fig. 4. The results show that the PbO_2 surface is smooth, while the composite surface shows roughness due to the presence of tiny TiO_2 crystals implanted in the PbO_2 layer [30]. In addition, we also see the surface morphology of coatings formed from particles with different sizes because

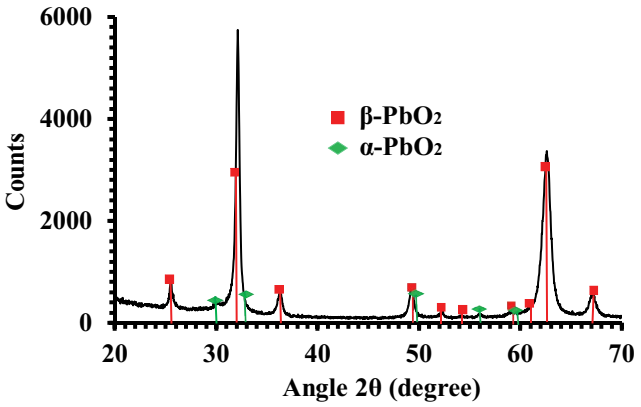

Fig. 2. XRD spectrum of SS/PbO_2-TiO_2 composite electrode (synthesized by CV method at 50 mV s^{-1}, 300 cycles).

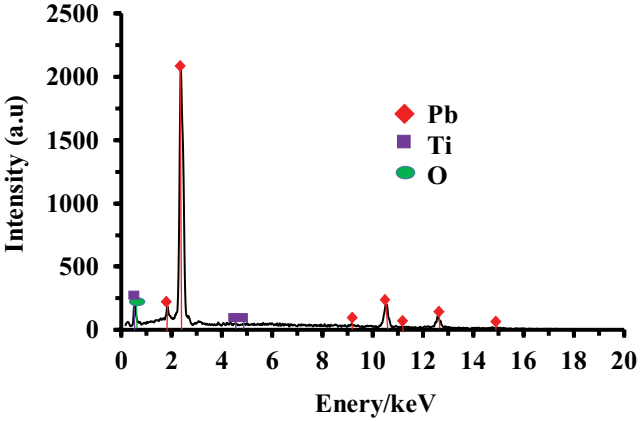

Fig. 3. EDS spectrum of PbO_2-TiO_2 composite (synthesized by CV method at 50 mV s^{-1}, 300 cycles).

Table 1
Rate of elements on the SS/PbO_2-TiO_2 composite electrode (synthesized at 50 mV s^{-1}, 300 cycles)

Element	Weight (%)	Atomic (%)
O K	24.35	80.44
Ti K	0.30	0.33
Pb M	75.35	19.23
Total	100.00	100.00

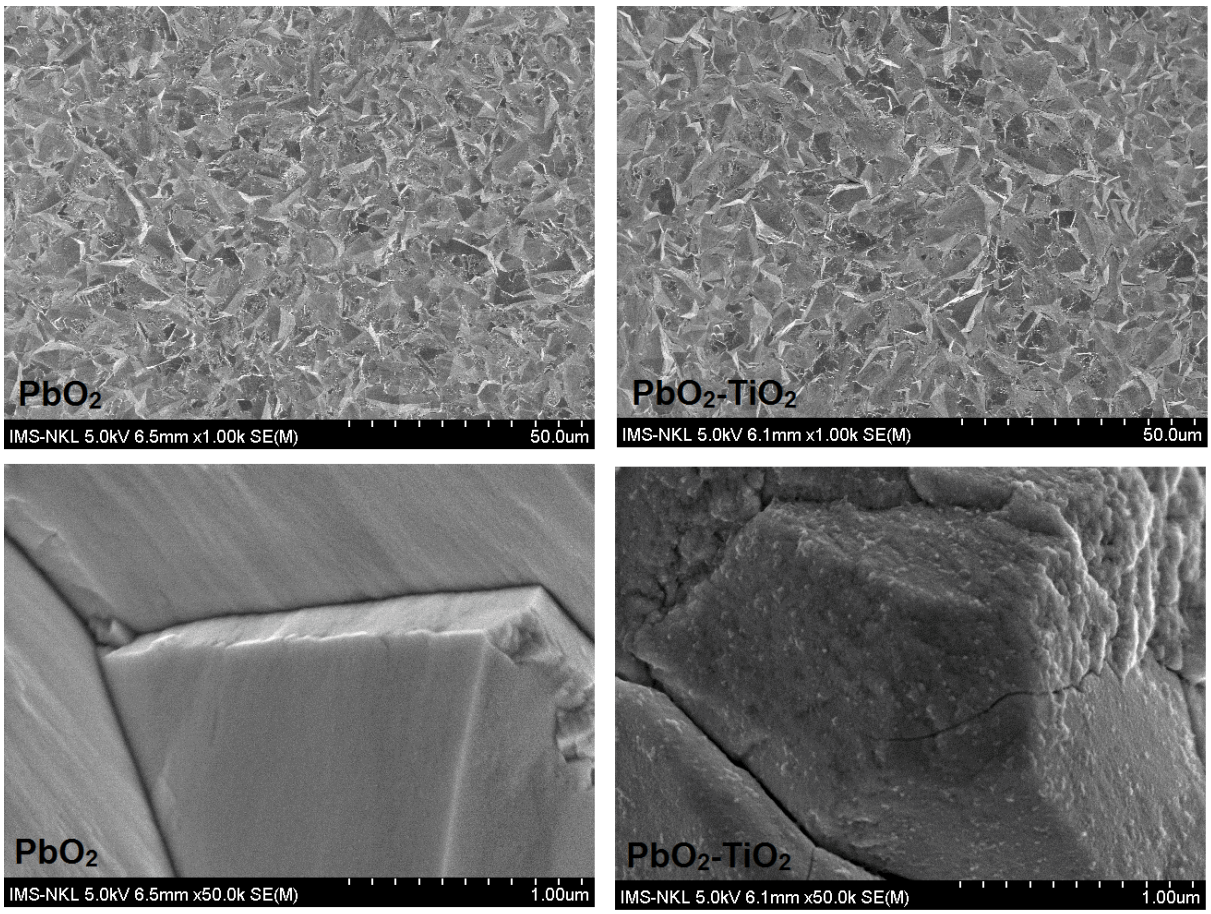

Fig. 4. SEM images of SS/PbO_2 (left side) and SS/PbO_2-TiO_2 composite (right side) electrodes (synthesized by CV method at 50 mV s^{-1}, 300 cycles).

PbO_2 existed in α- and β-modifications (orthorhombic and tetragonal, respectively) having different network parameters [35]. The particle size of PbO_2 on both coatings is almost the same and become compact together.

3.2. Electrochemical properties of SS/PbO_2-TiO_2 composite electrode

3.2.1. Cyclic voltammetry

Fig. 5 shows the voltammograms of SS/PbO_2-TiO_2 composite electrode in 0.5 M H_2SO_4 solution at a scan rate of 100 mV s^{-1}. On the 1st cycle, there was no oxidation peaks appeared but two reduction peaks were found corresponding to both α and β-modifications of lead dioxide to lead sulfate at 1.16 and 1.23 V, respectively. This indicates that both α- and β-PbO_2 forms exist together in the coating after electrode fabrication. This result is consistent with the XRD analysis above. From the 2nd cycle, only one reduction peak appeared indicating that this is the reduction peak of β-PbO_2 to $PbSO_4$. It increases following the CV number, however, its position was shifted lightly on the left side. From the 5th cycle the oxidation peaks demonstrated the formation

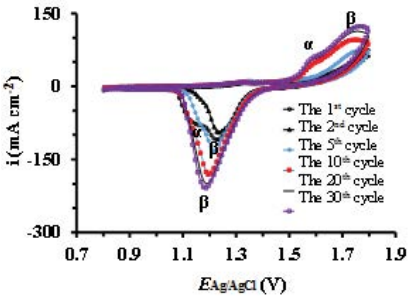

Fig. 5. Cyclic voltammograms of SS/PbO_2-TiO_2 composite electrode in 0.5 M H_2SO_4 at 100 mV s^{-1} (composite electrode synthesized by CV method at 50 mV s^{-1}, 300 cycles).

of α- and β-PbO_2 at about 1.60 and 1.75 V, respectively [36]. They were clearly increasing with CV number.

3.2.2. Potentiodynamic polarization

The potentiodynamic polarization curves of SS/PbO_2-TiO_2 composite and SS/PbO_2 electrodes in 0.5 M H_2SO_4 solution is shown in Fig. 6 from which the value of exchange

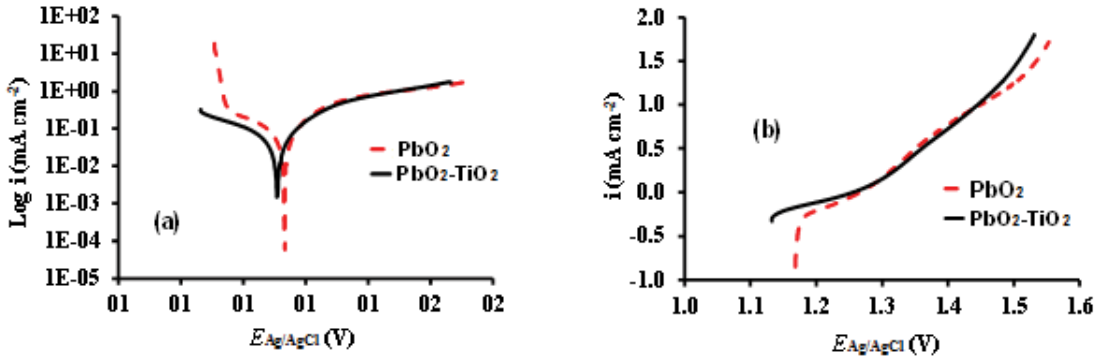

Fig. 6. Potentiodynamic polarization curves of SS/PbO_2 and SS/PbO_2-TiO_2 composite electrodes in 0.5 M H_2SO_4 at 5 mV s^{-1} in logarit (a) and in linear form (b) (composite electrode synthesized by CV method at 50 mV s^{-1}, 300 cycles).

current density of coating layers can be determined by the extrapolation of Tafel (Fig. 6a). If the exchange current density (ECD) is high, the surface of the electrode is more active [37,38]. This means that the both fabricated electrodes have a good catalytic ability for the electrochemical reaction occurring on their surface due to relatively high ECDs (61.8 and 53.4 μA cm^{-2} for PbO_2 and PbO_2-TiO_2 coatings, respectively). Linear graph (Fig. 6b) show that the composite electrode has slightly worse anodic polarization, but better cathodic polarization than PbO_2 electrode.

3.3. Treatment of MO

3.3.1. Research on MO decomposition mechanism

MO is treated by electrocatalytic oxidation processing. It means that the electrodegradation occurs on the surface of SS/PbO_2-TiO_2 anode electrode. HPLC/MS analysis results show that MO is fragmented into intermediate fragments before being decomposed into CO_2 and H_2O (Figs. 7 and 8). The electrochemical process can be described in detail below. The color of MO is mainly yellow thanks to the anion – SO_3^-. The proposed reaction mechanism for MO electrodegradation can be occurred in two steps. First, the hydroxyl radicals (•OH) formed by direct oxidation of water according to Eq. (2). They are physically adsorbed on the anode surface (AS) and become very active [21,29,39,40], which can oxidize organic compounds to intermediates following Eq. (3).

$$AS + H_2O \rightarrow AS(^{\bullet}OH) + H^+ + e^- \quad (2)$$

$$AS(^{\bullet}OH) + MO \rightarrow AS + \text{intermediates} \quad (3)$$

Second, MO is an oxidizable organic compounds so that the hydroxyl radicals will attack the electron-rich site such as –N=N– to decompose it being phenolic compounds (Fig. 8). These compounds further oxidized to quinone, organic carboxylic acid, and final products (CO_2 and H_2O) [11,14,40] as Eq. (4).

$$AS(^{\bullet}OH) + \text{intermediates} \rightarrow AS + CO_2 + H_2O + \text{inorganic ions} \quad (4)$$

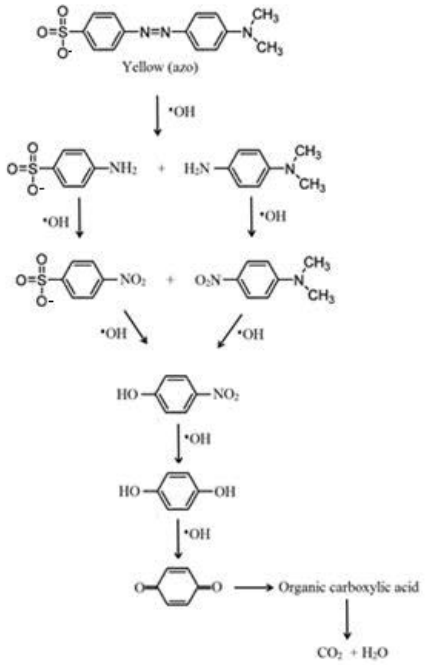

Fig. 7. Pathway of MO electrodegradation on anode electrode.

The OH radicals can be confirmed by tert-butanol as a quenching agent added to the MO solution before the electrochemical treatment begins. The results showed that the MO concentration after 10, 30 and 50 min of treatment reached 30.57, 20.60 and 13.53 mg L^{-1} in the presence of tert-butanol (0.08 M), respectively, higher than that of the solution without tert-butanol (27.53, 4.19 and 1.43 mg L^{-1}, respectively), from 50 mg L^{-1} initial MO concentration. It can be explained that some of the newly formed •OH radicals were quenched by tert-butanol [Eq. (5)] [41], so the ability to oxidize MO of the solution was less.

$$^{\bullet}OH + (CH_3)_3COH \rightarrow H_2O + CH_2C(CH_3)_2OH \quad (5)$$

3.3.2. The effect of current density

Current density is a very important factor in the electrochemical oxidation process. In the paper, current density

was used to remove MO from 1.0 to 2.0 mA cm^{-2}. Fig. 9a shows absorbance sharply decreases when current density increase. Fig. 9b shows that with MO initial concentration at 50 mg L^{-1} and treatment time of 60 min, the removal efficiency were achieved 86.84%, 94.25%, 96.43%, 97.55%, and 97.60% at the current density of 1.0, 1.25, 1.5, 1.75 and 2.0 mA cm^{-2}, respectively. The removal efficiency raises as the current density increase until 1.75 mA cm^{-2} (97.55%) and nearly unchanged at the current density of 2 mA cm^{-2} (97.60%). So current density of 1.75 mA cm^{-2} was used for the following studies.

3.3.3. The effect of treatment time

Different times (10, 20, 30, 40, 50 and 60 min) were applied to study the electrocatalytic MO degradation in solution (Fig. 10a and b). An increase in decolorization performance can be observed as the processing time is increased. However, the processing time increased from 50 to 60 min, the removal efficiency increased insignificantly at 97.15% and 97.55%, respectively. Therefore the optimal time for processing is 50 min.

3.3.4. The effect of initial concentration

The MO initial concentration ($C_{0,MO}$) is also a factor affecting the oxidation process. Therefore, in this paper, the MO initial concentration was considered from 30 to 100 mg L^{-1}. As the $C_{0,MO}$ increased, the absorbance increased (Fig. 11a) and the removal efficiency decreased (Fig. 11b). The optimal concentration is 50 mg L^{-1} with the efficiency of 97.15%.

3.3.5. The effect of solution pH

MO has two chemical structures corresponding to two different colors when the pH value of solution is different. If pH value is smaller than 4.4, MO has quinoid structure corresponding red color. When pH value is larger than 4.4, MO has azo structure corresponding yellow color [37]. Therefore, the effect of initial pH on MO degradation in wastewater was studied in the paper. The H_2SO_4 and NaOH solutions were used to adjust the solution pH [18]. Fig. 12a shows the absorbance reduces when pH reduces until 6 and is almost unchanged at pH of 5. So the suitable initial pH is 6. As can be seen from Fig. 12b, when initial pH increase from 5 until 7 the removal efficiency is very high (>99%), higher than that published in previous work using PbO_2-TiO_2 nanocomposite [27,28] and others [9–14,33,42] (Table 2). It indicates that MO molecules are easily decomposed at this pH range, but pH value larger than 7, the removal efficiency decreases sharply. Therefore, to be consistent with practice, a pH of 6 is the most suitable for MO treatment.

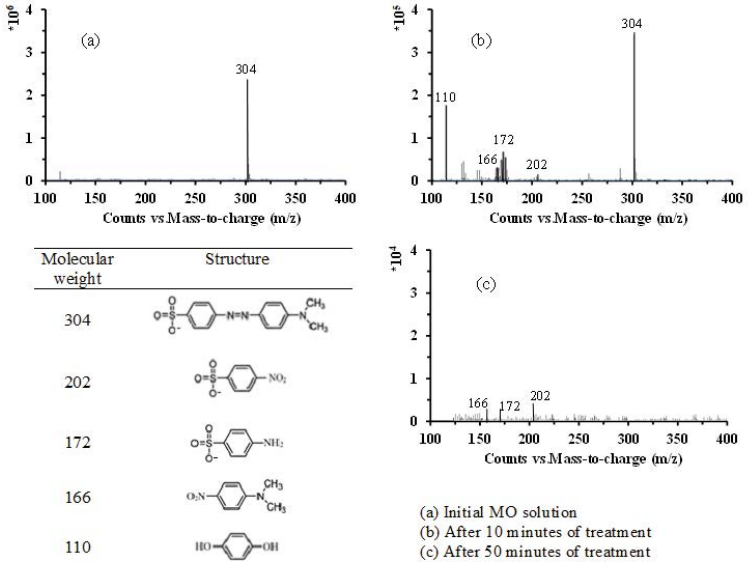

Fig. 8. HPLC/MS chromatographs before and after degradation of MO (C_{MO} of 50 mg L^{-1}, pH 6, current density of 1.75 mA cm^{-2}).

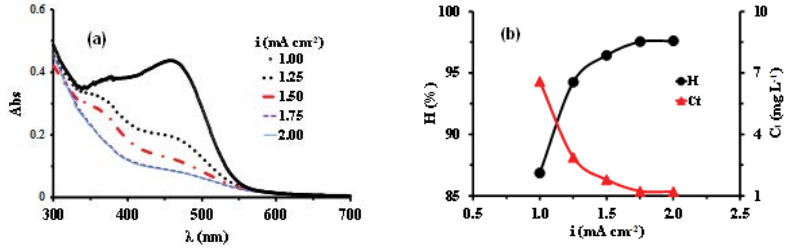

Fig. 9. UV-Vis spectra of the treated solution with different current densities (a); colour removal efficiency and residual MO concentration after 50 min at different current density from MO concentration of 50 mg L^{-1} (b) at pH 7.

From the results obtained in Fig. 13, the MO removal efficiency achieved after 50 min for the SS/PbO_2-TiO_2 composite electrode is 99.31%, higher than that of the SS/PbO_2 electrode (98.86%).

3.3.6. Kinetic study

The study of reaction rates has important implications for chemical processes. Therefore, the kinetic of MO degradation is considered in our research. The pseudo-first-order was applied to study the kinetics of MO decomposition with the following conditions: treatment time from 10 until 60 min, pH of 7, initial MO concentration of 50 mg L^{-1}, and current density of 1.75 mA cm^{-2}. The pseudo-first-order for MO degradation can be written as Eq. (6) [23,43,44] below:

$$\ln\left[\frac{C_o}{C_t}\right] = kt \quad (6)$$

where C_o and C_t are the MO concentrations before and after processing at time (t), respectively, and k is the constant of removal rate. The k can be determined from plot $\ln(C_o/C_t)$ vs. t (Fig. 14). The k of 0.0838 min^{-1} (R^2 = 0.9855) and 0.022 min^{-1} (R^2 = 0.9684) were found for the first period (0–40 min) and the second period (40–60 min), respectively. The MO processing speed in both periods is relatively linear because R^2 is quite high. However, this result also shows that the MO processing occurring at the first 40 min is almost four times faster than in the next stage.

3.3.7. Consideration of the ORP

As we know ORP is considered for indicating the level of MO solution treatment. The value of ORP can describe the quality of the solution, while the ΔORP between the inlet and outlet wastewater reflects the pollutant removal efficiency [45]. The higher the ORP value is, the better the

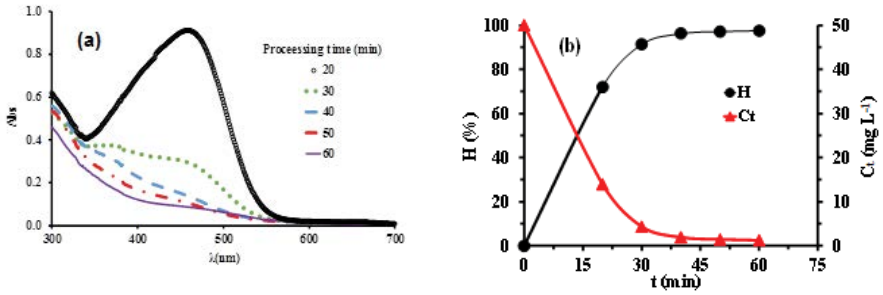

Fig. 10. UV-Vis spectra of the treated solution with different times (a); colour removal efficiency and residual MO concentration after different treatment time from MO concentration of 50 mg L^{-1} at pH 7.

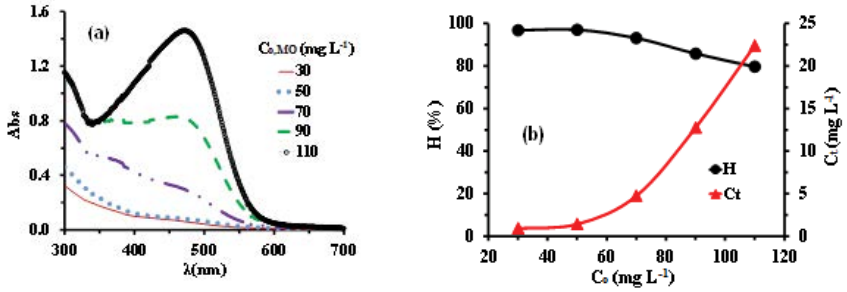

Fig. 11. UV-Vis spectra of the treated solution with different MO concentrations (a); colour removal efficiency and residual MO concentration after 50 min from different initial MO concentrations (b) at pH 7.

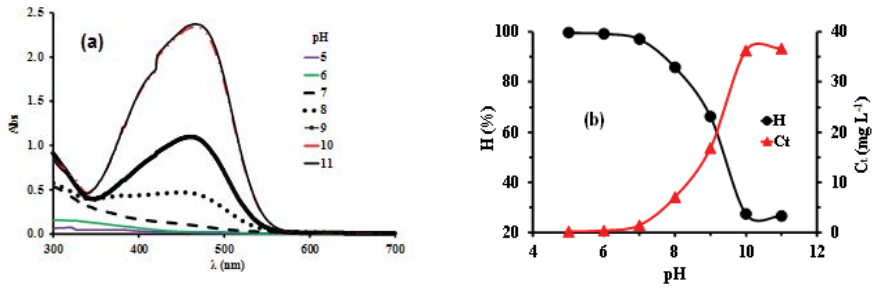

Fig. 12. UV-Vis spectra of treated solution with different pH (a); colour removal efficiency and residual MO concentration after 50 min treatment at different pH (b) from initial MO concentration of 50 mg L^{-1}.

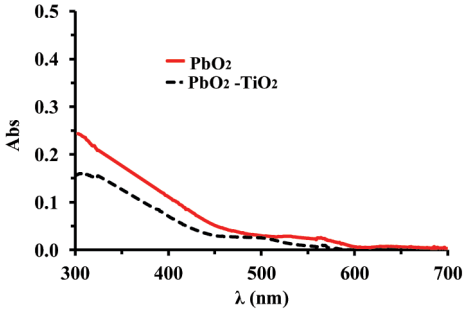

Fig. 13. UV-Vis spectra of treated solutions using SS/PbO_2 and SS/PbO_2-TiO_2 composite electrodes (treatment conditions: $C_{0,MO}$ of 50 mg L^{-1}, pH 6, 50 min at current density of 1.75 mA cm^{-2}).

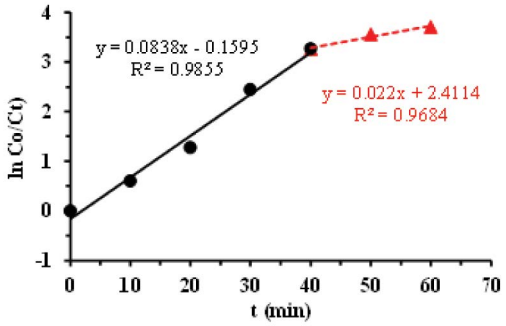

Fig. 14. The plots of ln(C_0/C_t) vs. MO treatment time *t*.

Table 2
Comparison of MO treatment with some published researches

Operating condition	Treatment method	Removal efficiency	References
Initial MO concentration of 100 ppm and a sorbent dose of 0.05 g, pH 3, temperature of 30°C	Using polymeric chitosan-*iso*-vanillin	97.9% after 3 h contact time	[9]
Initial MO concentration of 20 mg L^{-1} and pH 6	Using hog plum peel and mix-bacterial strains	92.0% after 60 min contact time	[10]
Initial MO concentration of 100 mg L^{-1} in 1 g L^{-1} synthesized nano-zinc oxide and 1.5 g L^{-1} sodium persulfate, pH 6.5	By sonophotocatalytic treatment with synthesized nano-zinc oxide	84.0% after reaction time of 60 min	[11]
[MO] = 5.4 × 10^{-5} M, [Fe^{2+}] = 1.9 × 10^{-4} M; [H_2O_2] = 2.93 × 10^{-3} M; pH = 2.79 at room temperature	By Fenton reaction	97.8% after 15 min	[12]
Iron electrode (22.5 cm^2) as an active surface, current density of 64 A m^{-2}, and pH 7.25	By electrocoagulation	83.0% after 15 min processing	[13]
Ti_4O_7 electrode as anode, current density of 10 mA cm^{-2}, initial MO concentration of 150 mg L^{-1}, NaCl of 0.01 M	By electrocatalytic oxidation	98.2% after 30 min processing	[14]
Ti/SnO_2-Sb/PbO_2-TiO_2 nanocomposite electrode as anode, initial MO concentration of 50 mg L^{-1}	By electrocatalytic oxidation	66.4% after 2 h at constant potential	[27]
Ti/SnO_2-Sb_2O_3/PbO_2-TiO_2 nanocomposite electrode as anode in 0.1 mol L^{-1} Na_2SO_4 solution containing 30 mg L^{-1} MO with current density of 30 mA cm^{-2}	By electrocatalytic oxidation	95.5% after 240 min processing	[28]
Pt electrode as anode for electrocatalysis	By self-powered electrocatalytic oxidation	80.0% after 144 h treatment	[42]
Pressure of 0.4 MPa, temperature of 35°C, chlorine dioxide concentration of 8 mg L^{-1}, pH from 3 to 9	By combining hydrodynamic cavitation and chlorine dioxide treatments	90.5% after reaction time of 90 min	[33]
SS/PbO_2-TiO_2 composite electrode as anode, pH6, initial MO concentration of 50 mg L^{-1}, current density of 1.75 mA cm^{-2}	By electrocatalytic oxidation	99.31% after 50 min processing	Our research

Table 3
Comparison of several results regarding ORP values in the presence of tert-butanol

Treatment time (min)	Tert-butanol (M)	pH	ORP (mV)	ΔORP (mV)	MO removal efficiency (%)
0	0	5.98	172.6	0	0
10	0.08	6.31	411.2	238.6	38.87
10	0	6.45	419.4	246.8	44.94
30	0.08	6.37	421.1	248.5	58.79
30	0	6.39	447.8	275.2	91.62
50	0.08	6.40	432.7	260.1	72.94
50	0	6.48	452.8	280.2	99.31

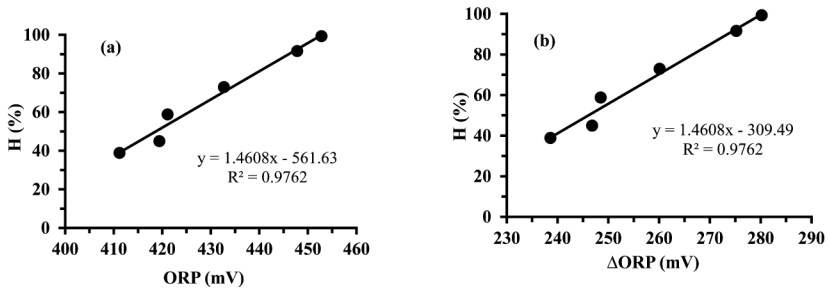

Fig. 15. Relationship between ORP and *H* (a), ΔORP and *H* (b).

oxidation state of the solution is. The higher the ΔORP value is, the higher the pollutant removal efficiency is. ORP results also can help us predict the oxidation state of ions in solution and whether certain reactions are possible. The results in Table 3 show that all detected ORP values are positive (172.6–452.8 mV), indicating that the solution is capable of oxidizing. Fig. 15 shows that the relationship between ORP and *H* (a), ΔORP and *H* (b) is linear with the same correlation coefficient of 0.9762, nearly independent of the presence of tert-butanol.

4. Conclusion

The PbO_2-TiO_2 layer can be synthesized directly on the SS substrate by CV method easily, achieving a dense surface and good electrocatalytic ability in MO treatment from solution. MO processing occurs in two stages at different rates, of which the first stage lasted 40 min (k = 0.0838 min^{-1}), which is almost four times faster than the next stage (20 min; k = 0.022 min^{-1}). The MO removal efficiency is almost complete after 50 min, reaching 99.31% under optimal processing conditions (current density of 1.75 mA cm^{-2}, treatment time of 50 min, initial methylene orange concentration of 50 mg L^{-1} and pH 6). The SS/PbO_2-TiO_2 stable electrode is an effective anodic material for MO degradation and promising for the electrocatalytic oxidation of other organic pollutants in wastewater. However, the cost of MO processing has not been considered in this study.

Abbreviations

AS	—	Anode surface
CV	—	Cyclic voltammetry
ECD	—	Exchange current density
EDS	—	Energy dispersive X-ray spectroscopy
HPLC/MS	—	High-pressure liquid chromatography-mass spectrometry
MO	—	Methyl orange
OCP	—	Open circuit voltage
ORP	—	Oxidation–reduction potential
SEM	—	Scanning electron microscope
SS	—	Stainless steel
UV-Vis	—	Ultraviolet Visible
XRD	—	X-ray diffraction

References

[1] M.R. Samarghandi, A. Dargahi, A. Shabanloo, H.Z. Nasab, Y. Vaziri, A. Ansari, Electrochemical degradation of methylene blue dye using a graphite doped PbO_2 anode: optimization of operational parameters, degradation pathway and improving the biodegradability of textile wastewater, Arabian J. Chem., 13 (2020) 6847–6864.
[2] M.R. Samarghandi, A. Dargahi, H.Z. Nasab, E. Ghahramani, S. Salehi, Degradation of azo dye Acid Red 14 (AR14) from aqueous solution using H_2O_2/nZVI and $S_2O_8^{2-}$/nZVI processes in the presence of UV irradiation, Water Environ. Res., 92 (2020) 1173–1183.
[3] A. Peyghami, A. Moharrami, Y. Rashtbari, S. Afshin, M. Vosuoghi, A. Dargahi, Evaluation of the efficiency of magnetized clinoptilolite zeolite with Fe_3O_4 nanoparticles on the removal of basic violet 16 (BV16) dye from aqueous solutions, J. Dispersion Sci. Technol., (2021) 1947847, doi: 10.1080/01932691.2021.1947847.
[4] M.M. Nassar, Y.H. Magdy, Removal of different basic dyes from aqueous solutions by adsorption on palm-fruit bunch particles, Chem. Eng. J., 66 (1997) 223–226.
[5] H. Zou, Y. Wang, Functional collaboration of biofilm-cathode electrode and microbial fuel cell for biodegradation of methyl orange and simultaneous bioelectricity generation, Environ. Sci. Pollut. Res., 26 (2019) 23061–23069.
[6] M. Koyuncu, Removal of Maxilon Red GRL from aqueous solutions by adsorption onto silica, Orient. J. Chem., 25 (2009) 35–40.
[7] M.Z.B. Mukhlish, M.R. Khan, A.R. Islam, A.N.M.S. Akanda, Removal of reactive dye from aqueous solution using coagulation–flocculation coupled with adsorption on papaya leaf, J. Mech. Eng. Sci. (JMES), 1 (2016) 1884–1894.
[8] X.Z. Li, Y.G. Zhao, On-site treatment of dyeing wastewater by a bio-photoreactor system, Water Sci. Technol., 36 (1997) 165–172.
[9] E.A. Alabbad, Efficient removal of methyl orange from wastewater by polymeric chitosan-*iso*-vanillin, Open Chem. J., 7 (2020) 16–25.
[10] J.F. Rumky, Z. Abedin, H. Rahman, M. Ali Hossain, Environmental treatment of dyes: methyl orange decolorization using hog plum peel and mix-bacterial strains, IOSR-JESTFT, 5 (2013) 19–22.
[11] R. Hemapriyamvadha, T. Sivasankar, Sonophotocatalytic treatment of methylorange dye and real textile effluent using synthesised nano-zinc oxide, Color Technol., 131 (2015) 1–10.
[12] N.A. Youssef, S.A. Shaban, F.A. Ibrahim, A.S. Mahmoud, Degradation of methyl orange using Fenton catalytic reaction, Egypt. J. Petrol., 25 (2016) 317–321.
[13] S. Irki, D. Ghernaout, M.W. Naceur, A. Alghamdi, M. Aichouni, Decolorizing methyl orange by Fe-electrocoagulation process – a mechanistic insight, Int. J. Environ. Chem., 2 (2018) 18–28.
[14] G. Wang, Y. Liu, J. Ye, Z. Lin, X. Yang, Electrochemical oxidation of methyl orange by a Magnéli phase Ti_4O_7 anode, Chemosphere, 241 (2020) 125084, doi: 10.1016/j.chemosphere.2019.125084.
[15] M. Roy, R. Saha, Chapter 6 – Dyes and Their Removal Technologies From Wastewater: A Critical Review, S. Bhattacharyya, J. Platos, P. Krömer, N.K. Mondal, V. Snášel, Eds., Intelligent Environmental Data Monitoring for Pollution Management: Intelligent Data-Centric Systems, Academic Press, 2021, pp. 127–160.
[16] Y. Yao, C. Zhao, M. Zhao, X. Wang, Electrocatalytic degradation of methylene blue on PbO_2-ZrO_2 nanocomposite electrodes prepared by pulse electrodeposition, J. Hazard. Mater., 263 (2013) 726–734.

[17] L. Ciríaco, C. Anjo, J. Correia, M.J. Pacheco, A. Lopes, Electrochemical degradation of ibuprofen on Ti/Pt/PbO_2 and Si/BDD electrodes, Electrochim. Acta, 54 (2009) 1464–1472.
[18] H. Yang, J. Liang, L. Zhang, Z. Liang, Electrochemical oxidation degradation of methyl orange wastewater by Nb/PbO_2 electrode, Int. J. Electrochem. Sci., 11 (2016) 1121–1134.
[19] A. Dargahi, M. Vosoughi, S. Ahmad Mokhtari, Y. Vaziri, M. Alighadri, Electrochemical degradation of 2,4-Dinitrotoluene (DNT) from aqueous solutions using three-dimensional electrocatalytic reactor (3DER): degradation pathway, evaluation of toxicity and optimization using RSM-CCD, Arabian J. Chem., 15 (2022) 103648, doi: 10.1016/j.arabjc.2021.103648.
[20] M.R. Samarghandi, A. Dargahi, A. Rahmani, A. Shabanloo, A. Ansari, D. Nematollahi, Application of a fluidized three-dimensional electrochemical reactor with Ti/SnO_2–Sb/β-PbO_2 anode and granular activated carbon particles for degradation and mineralization of 2,4-dichlorophenol: process optimization and degradation pathway, Chemosphere, 279 (2021) 130640, doi: 10.1016/j.chemosphere.2021.130640.
[21] M.R. Samarghandi, A. Ansari, A. Dargahi, A. Shabanloo, D. Nematollahi, M. Khazaei, H.Z. Nasab, Y. Vaziri, Enhanced electrocatalytic degradation of bisphenol A by graphite/β-PbO_2 anode in a three-dimensional electrochemical reactor, J. Environ. Chem. Eng., 9 (2021) 106072, doi: 10.1016/j.jece.2021.106072.
[22] Z.A. Jonoush, A. Rezaee, A. Ghaffarinejad, Enhanced electrocatalytic denitrifcation using non-noble Ni-Fe electrode supplied by Fe_3O_4 nanoparticle and humic acid, Appl. Surf. Sci., 563 (2021) 150142, doi: 10.1016/j.apsusc.2021.150142.
[23] M.M. Mahmoudi, R. Khaghani, A. Dargahi, G. Monazami Tehrani, Electrochemical degradation of diazinon from aqueous media using graphite anode: effect of parameters, mineralisation, reaction kinetic, degradation pathway and optimisation using central composite design, Int. J. Environ. Anal. Chem., 102 (2020) 1709–1734.
[24] A. Dargahi, A. Ansari, D. Nematollahi, G. Asgari, R. Shokoohi, M.R. Samarghandi, Parameter optimization and degradation mechanism for electrocatalytic degradation of 2,4-diclorophenoxyacetic acid (2,4-D) herbicide by lead dioxide electrodes, RSC Adv., 9 (2019) 5064–5075.
[25] N.M. Abu Ghalwa, F.R. Zaggout, Electrodegradation of methylene blue dye in water and wastewater using lead oxide/titanium modified electrode, J. Environ. Sci. Health. Part A Toxic/Hazard. Subst. Environ. Eng., 41 (2006) 2271–2282.
[26] S. Yuzhu, C. Zhen, G. Lai, Y. Qiang, Z. Wei, W. Dan, Z. Tao, Fabrication and electrocatalytic performance of a two-dimensional β-PbO_2 macroporous array for methyl orange degradation, Int. J. Electrochem. Sci., 14 (2019) 7790–7810.
[27] H. Xu, Q. Zhang, W. Yan, W. Chu, L. Zhang, Preparation and characterization of PbO_2 electrodes doped with TiO_2 and its degradation effect on azo dye wastewater, Int. J. Electrochem. Sci., 8 (2013) 5382–5395.
[28] Y.W. Yao, L.H. Cui, Y. Li, N.C. Yu, H.S. Dong, X. Chen, F. Wei, Electrocatalytic degradation of methyl orange on PbO_2-TiO_2 nanocomposite electrodes, Int. J. Environ. Res., 9 (2015) 1357–1364.
[29] L. Zhu, Y. Tian, M. Li, H. Ma, C. Ma, X. Dong, X. Zhang, Fabrication and photo-electrocatalytic activity of black TiO_2 embedded Ti/PbO_2 electrode, J. Appl. Electrochem., 47 (2017) 1045–1056.
[30] A.B. Velichenko, V.A. Knysh, T.V. Luk'yanenko, F.I. Danilov, D. Devilliers, PbO_2–TiO_2 composite electrodes, Prot. Met. Phys. Chem., 45 (2009) 327–332.
[31] R. Amadelli, L. Samiolo, A.B. Velichenko, V.A. Knysh, T.V. Luk'yanenko, F.I. Danilov, Composite PbO_2–TiO_2 materials deposited from colloidal electrolyte: electrosynthesis, and physicochemical properties, Electrochim. Acta, 54 (2009) 5239–5245.
[32] A.B. Velichenko, V.A. Knysh, T.V. Luk'yanenko, N.V. Nikolenko, Electrodeposition of PbO_2–TiO_2 nanocomposite materials from suspension electrolytes, Theor. Exp. Chem., 52 (2016) 127–131.
[33] S. Yang, R. Jin, Z. He, Y. Qiao, S. Shi, W. Kong, Y. Wang, X. Liu, An experimental study on the degradation of methyl orange by combining hydrodynamic cavitation and chlorine dioxide treatments, Chem. Eng. Trans., 59 (2017) 289–294.
[34] P.T. Tot, M.T.T. Thuy, N.T. Duyen, P.T. Binh, Synthesis and study on characterization of PbO_2 on stainless steel, J. Sci., 69 (2020) 27–34.
[35] J.P. Carr, N.A. Hampson, The lead dioxide electrode, Chem. Rev., 72 (1972) 679–702.
[36] P.T. Binh, M.T.T. Thuy, Characterization of PbO_2 synthesized by current pulse method on stainless steel, Vietnam J. Chem., 47 (2009) 60–65.
[37] N. Mohammadi, M. Yari, S.R. Allahkaram, Characterization of PbO_2 coating electrodeposited onto stainless steel 316L substrate for using as PEMFC's bipolar plates, Surf. Coat. Technol., 236 (2013) 341–346.
[38] H. Ma, B. Wang, X. Luo, Studies on degradation of methyl orange wastewater by combined electrochemical process, J. Hazard. Mater., 149 (2007) 492–498.
[39] S. Siahrostami, G.-L. Li, V. Viswanathan, J.K. Norskov, One- or two-electron water oxidation, hydroxyl radical or H_2O_2 evolution, J. Phys. Chem. Lett., 8 (2017) 1157–1160.
[40] S. Klamklang, H. Vergnes, K. Pruksathorn, S. Damronglerd, Electrochemical Incineration of Organic Pollutants for Wastewater Treatment: Past, Present and Prospect, T. Puzyn, A. Mostrag-Szlichtyng, Eds., Organic Pollutants Ten Years After the Stockholm Convention – Environmental and Analytical Update, InTechOpen, 2012, pp. 365–382.
[41] B. Ervens, S. Gligorovski, H. Herrmann, Temperature-dependent rate constants for hydroxyl radical reactions with organic compounds in aqueous solutions, Phys. Chem. Chem. Phys., 5 (2003) 1811–1824.
[42] Y. Yang, H. Zhang, S. Lee, D. Kim, W. Hwang, Z.L. Wang, Hybrid energy cell for degradation of methyl orange by self-powered electrocatalytic oxidation, Nano Lett., 13 (2013) 803–808.
[43] A. Dargahi, M.M. Samarghandi, A. Shabanloo, M.M. Mahmoudi, H.Z. Nasab, Statistical modeling of phenolic compounds adsorption onto low-cost adsorbent prepared from aloe vera leaves wastes using CCD-RSM optimization: effect of parameters, isotherm, and kinetic studies, Biomass Convers. Biorefin., (2021), doi: 10.1007/s13399-021-01601-y.
[44] R. Shokoohi, A. Dargahi, R.A. Gilan, H.Z. Nasab, D. Zeynalzadeh, M.M. Mahmoudi, Magnetic multi-walled carbon nanotube as effective adsorbent for ciprofloxacin (CIP) removal from aqueous solutions: isotherm and kinetics studies, Int. J. Chem. Reactor Eng., 18 (2019), doi: 10.1515/ijcre-2019-0130.
[45] Yokogawa Company, pH and ORP Learning Handbook, 2014, pp. 28–33.